

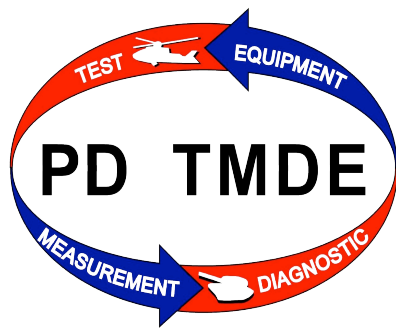
Accounting for the Impact of Thermal Instability in the Liquid Comprising the Connecting Volume of a Piston Displacement type Volumetric Flow Rate Standard

A Technical Paper Produced as part of the Joint Army & Air Force Metrology Research & Development Project CCG-576

Authors: Jeremy Latsko AFMETCAL and James Winchester AEDC Arnold AFB

Army Team Lead: Judy Burden

Army Team Members: John Ball, Wes England, Russell Kaufmann, Michael Vickers & Greg Rigney



Air Force Team Lead: Jeremy Latsko

Air Force Team Members: James Winchester & 2nd Lt. William Parker



University of Tennessee Space Institute

Joel Davenport



Accounting for the Impact of Thermal Instability in the Liquid Comprising the Connecting Volume of a Piston Displacement type Volumetric Flow Rate Standard

Speaker: Jeremy Latsko
Air Force Metrology and Calibration (AFMETCAL)
813 Irving-Wick Dr. W. Bldg 2
Heath, OH 43056-1199
Phone: (740) 788-5128 Fax: (740) 788-5012
jeremy.latsko@afmetcal.af.mil

Authors: Jeremy Latsko (AFMETCAL), James Winchester (Arnold Engineering Development Center, Arnold Air Force Base, Tennessee)

Abstract

The Air Force uses conventional pumped fluid piston displacement volumetric flow rate standards which employ an equation provided by the manufacturer for determining average volumetric flow rate through the meter under test during standard volume delivery. The Air Force's calibrators are operated assuming that steady state thermal conditions are achieved throughout the fluid residing in the connecting volume between the metering piston and the meter under test during standard volume delivery. Accordingly, this assumption implies that the net gain/loss of thermal energy – and therefore any decrease/increase in volumetric flow as a result of fluid contraction/expansion – is negligible to the system's overall uncertainty. Using a specially instrumented flow calibrator, the effects of not accounting for thermal instabilities have been analyzed and quantified. Based on these data, it is believed that true thermal stability is not practically achieved. Further, not accounting for thermal instabilities can result in an increase in overall flow rate uncertainty, most notably at lower flow rates. The consequence is the degraded uncertainty, changes to established procedures which can add time and cost to calibrations, or a reduction in the large turndowns over which these calibrators are often operated.

We propose the use of the complete volume flow rate equation – accounting for the fluid in the connecting volume – in order to achieve stated uncertainties derived under the assumption of thermal stability. To implement this change, new instrumentation must be added which includes both a means for measuring fluid temperature throughout the connecting volume and for measuring the absolute position of the metering piston in the cylinder at the conclusion of a standard volume delivery.

The technical paper on this topic will detail the theories employed, calibrator modifications, studies conducted, and resultant conclusions. It will also ultimately provide the reader with actionable information to improve piston displacement standard flow rate measurements over large turndowns.

Introduction

The United States Air Force calibrates liquid flowmeters for use in turbine engine research and development testing, engine evaluation after rebuild, etc. These flowmeters are calibrated using piston displacement type volumetric flow rate standards, which have been in use for many years.

Over the last several years, the Air Force has begun plans to modernize these standards – controllers, software, etc. Amidst these conversations, we began to discuss possible metrological shortfalls with the existing standards. Of primary concern was the notion of assuming that thermal stability/steady state conditions are always achieved during standard volume delivery to the meter under test. Further, if thermal instabilities exist during a standard volume delivery, how do we account for this knowing that its effect on delivered flow rate is a function of the connecting volume (as defined by the fluid between the metering piston and the meter under test), when the metering piston absolute position in the cylinder is currently not measured as required to determine the total connecting volume?

Early on, a simple test was conducted to monitor fluid temperature at the cylinder discharge and at the meter under test. Temperature control was set to 80 °F with a variety of flow rate settings. Figure 1 shows the temperature variations observed over the course of 60 minutes. The method utilized to collect these data was not optimal in that we taped measurement probes to the exterior of connecting volume piping; however, the data showed that thermal stability was likely not being achieved and prompted further investigation.

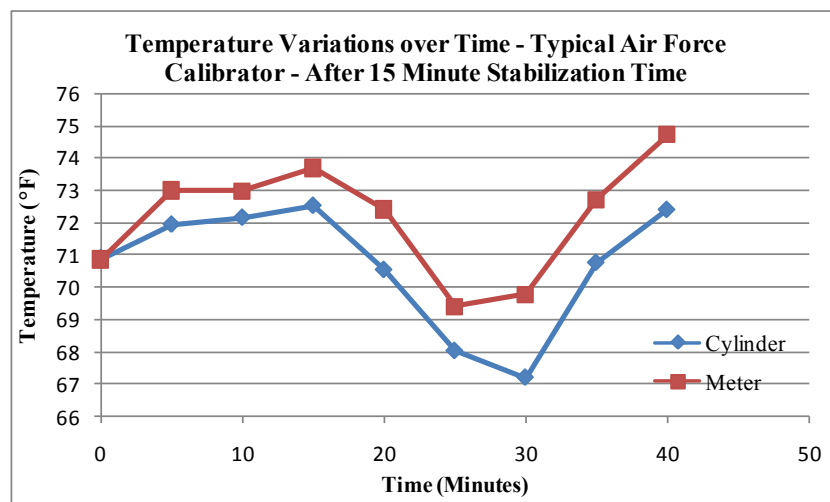


Figure 1: Temperature variability over time.

Knowing this, nominal data was used to explore the error associated with not accounting for thermal instabilities. The results are reported in Table 1. Quantification of the error uses the characteristics of a typical 350 GPM calibrator using Stoddard Solvent at 5 GPM and assumes the worst case scenario where the metering piston begins delivery of flow at the beginning of the cylinder (i.e. as far away as possible from the cylinder discharge end). Depending on the

uncertainty analysis for the particular calibrator, these errors may be in addition to the stated uncertainty for a calibrator that assumes thermal stability has been achieved during data collection. This is ultimately based on the manufacturer’s uncertainty analysis. The values below are based on the equation for average volumetric flow rate at the meter under test as derived in this paper.

	Case #1	Case #2	Case #3	Case #4
Standard Volume Delivery Time (minutes)	1	1	0.25	0.25
Ratio of Connecting Volume to Standard Volume	11.2	11.2	47.8	47.8
Spatial Temperature Difference Between Start and End of Standard Volume Delivery (°F)	0.025	0.05	0.025	0.05
Error Associated with Assuming Steady State	0.015%	0.031%	0.066%	0.132%

Table 1: Estimated flow rate errors associated with thermal instabilities.

Despite the cursory test and error determination, we believed that errors will exist even with a slight difference in spatial average temperature between the start and end of a standard volume delivery, as Case #3 indicates when there is a difference of only 0.025 °F. In other words, thermal instabilities can ultimately lead to degraded flow rate measurement uncertainty. We knew that further – more thorough testing – needed to be conducted to study and truly quantify these effects.

First, however, we develop the relationship for average volumetric flow rate delivered to the meter under test, where from these errors were derived.

Derivation of Equation for Average Volumetric Flow Rate Delivered to Meter Under Test

Piston displacement liquid flow calibration systems in the Air Force inventory employ the following equation to derive flow rate at the meter under test from flow rate delivered by the displacement of the metering piston.

$$\bar{V}_{MUT} = \bar{V}_{STD} \cdot \frac{\bar{\rho}_{STD}}{\bar{\rho}_{MUT}}$$

This equation was derived from conservation of mass principles and the assumption that the mass of fluid flowing through the meter under test during the standard volume delivery equals the mass of the fluid discharged in the standard volume.

$$M_{MUT} = M_{STD}$$

Given that volume equals mass divided by density,

$$V = M/\rho,$$

average volumetric flow rate, \bar{V} , is equal to the total volume delivered divided by time of delivery, t_c . Dividing both sides of the equation above by t_c then yields

$$\frac{V}{t_c} = \frac{M}{\rho \cdot t_c} = \bar{V}$$

Given that a period of time is involved in this determination and knowing that a fluid density can vary, the density term should be the temporal average density during the time period considered for this equation to be true.

$$\bar{V} = \frac{M}{\bar{\rho} \cdot t_c}$$

We can look now at the two volumetric flow rates of interest,

$$\bar{V}_{STD}, \text{ and } \bar{V}_{MUT}.$$

Remembering that at this point we are working under the assumption that mass out of the standard equals mass through the meter under test,

$$\bar{V}_{STD} = \frac{M}{\bar{\rho}_{STD} \cdot t_c}$$

And

$$\bar{V}_{MUT} = \frac{M}{\bar{\rho}_{MUT} \cdot t_c}$$

The ratio of these two equations is considered below

$$\frac{\bar{V}_{MUT}}{\bar{V}_{STD}} = \left(\frac{1}{t_c} \cdot \frac{M}{\bar{\rho}_{MUT}} \right) / \left(\frac{1}{t_c} \cdot \frac{M}{\bar{\rho}_{STD}} \right) = \frac{\bar{\rho}_{STD}}{\bar{\rho}_{MUT}}$$

From which we do readily derive

$$\bar{V}_{MUT} = \bar{V}_{STD} \cdot \frac{\bar{\rho}_{STD}}{\bar{\rho}_{MUT}}$$

Again, the above equation is derived assuming that the mass of fluid in the delivered standard volume equals the mass of fluid passing through the meter under test during the delivery of the standard volume. In reality, this assumption is a simplification which ignores the impact of a

connecting volume filled with a mass of fluid prior to and after the delivery of a standard volume. The conservation of mass principle actually dictates that the mass of fluid delivered in the standard volume plus the mass of fluid in the connecting volume at the initiation of standard volume delivery equals the mass of fluid passing through the meter under test during the standard volume delivery plus the mass of fluid in the connecting volume at the completion of standard volume delivery.

$$M_{STD} + M_{CVi} = M_{MUT} + M_{CVf}$$

From this equation we can derive an improved equation for the flow rate at the meter under test relative to the flow rate from the standard during the delivery of the standard volume.

Given that mass equals density times volume, $M = \rho \cdot V$, the mass in a volume delivered over a period of time equals the temporal average density of the fluid passing from the delivery process during the delivery multiplied by the volume delivered and the mass through the meter under test equals the temporal average density of the fluid passing through multiplied by the volume of that fluid. In the case of initial and final mass in the connecting volume, these are equal to the “snap shot” spatial average density at the start and at the finish of standard volume delivery multiplied by the connecting volume.

$$\bar{\rho}_{STD} \cdot V_{STD} + \rho_{CVi} \cdot V_{CV} = \bar{\rho}_{MUT} \cdot V_{MUT} + \rho_{CVf} \cdot V_{CV}$$

Since we wish to eventually know flow rates and we are measuring the time of standard volume delivery, t_c , we can divide both sides of the above equation by this factor.

$$\frac{\bar{\rho}_{MUT} \cdot V_{MUT}}{t_c} = \frac{\bar{\rho}_{STD} \cdot V_{STD}}{t_c} + \frac{\rho_{CVi} \cdot V_{CV} - \rho_{CVf} \cdot V_{CV}}{t_c}$$

Flow rate through the meter under test can be isolated on the left hand side of the equation by dividing both sides by the average density through the meter under test, $\bar{\rho}_{MUT}$.

$$\frac{V_{MUT}}{t_c} = \frac{\bar{\rho}_{STD} \cdot V_{STD}}{\bar{\rho}_{MUT} \cdot t_c} + \frac{V_{CV} \cdot (\rho_{CVi} - \rho_{CVf})}{\bar{\rho}_{MUT} \cdot t_c}$$

The average flow rate at the meter under test during standard volume delivery is equal to the volume delivered divided by the time of delivery and expressed here as \bar{V}_{MUT} . From the above expression

$$\bar{V}_{MUT} = \frac{\bar{\rho}_{STD} \cdot V_{STD}}{\bar{\rho}_{MUT} \cdot t_c} + \frac{V_{CV} \cdot (\rho_{CVi} - \rho_{CVf})}{\bar{\rho}_{MUT} \cdot t_c}$$

Similarly, the average flow rate from the standard is equal to the standard volume divided by the time of delivery and is present in the first term of the right hand side of the equation above which can be expressed as below.

$$\bar{V}_{MUT} = \bar{V}_{STD} \cdot \frac{\bar{\rho}_{STD}}{\bar{\rho}_{MUT}} + \frac{V_{CV} \cdot (\rho_{CV_i} - \rho_{CV_f})}{\bar{\rho}_{MUT} \cdot t_c}$$

If we divide the second term of the right hand side of the above equation by \bar{V}_{STD} , we can then combine both right hand side terms as multiplies of \bar{V}_{STD} resulting in the following equation.

$$\bar{V}_{MUT} = \bar{V}_{STD} \cdot \left[\frac{\bar{\rho}_{STD}}{\bar{\rho}_{MUT}} + \frac{V_{CV} \cdot (\rho_{CV_i} - \rho_{CV_f})}{\bar{V}_{STD} \cdot \bar{\rho}_{MUT} \cdot t_c} \right]$$

Given that $\bar{V}_{STD} = V_{STD}/t_c$, we can further refine the equation as noted below

$$\bar{V}_{MUT} = \bar{V}_{STD} \cdot \left[\frac{\bar{\rho}_{STD}}{\bar{\rho}_{MUT}} + \frac{V_{CV} \cdot (\rho_{CV_i} - \rho_{CV_f})}{V_{STD} \cdot \bar{\rho}_{MUT}} \right]$$

Which reduces to,

$$\bar{V}_{MUT} = \bar{V}_{STD} \cdot \left[\frac{\bar{\rho}_{STD}}{\bar{\rho}_{MUT}} + \frac{V_{CV}}{V_{STD}} \cdot \frac{(\rho_{CV_i} - \rho_{CV_f})}{\bar{\rho}_{MUT}} \right]$$

For clarity in the next steps this can be expressed as below,

$$\bar{V}_{MUT} = \bar{V}_{STD} \cdot \left[\frac{\bar{\rho}_{STD}}{\bar{\rho}_{MUT}} + \frac{V_{CV}}{V_{STD}} \cdot \left(\frac{\rho_{CV_i}}{\bar{\rho}_{MUT}} - \frac{\rho_{CV_f}}{\bar{\rho}_{MUT}} \right) \right]$$

In a fluid of given thermal expansion coefficient, β , the ratio of density at different temperatures, T_A & T_B can be expressed as below

$$\frac{\rho_{T_A}}{\rho_{T_B}} = 1 + \beta \cdot (T_B - T_A)$$

During a period of time, t_c , the ratio of average densities over the period would be determined using the temporal average temperatures.

$$\frac{\bar{\rho}_{STD}}{\bar{\rho}_{MUT}} = 1 + \beta \cdot (\bar{T}_{MUT} - \bar{T}_{STD})$$

For determining the initial and final densities of fluid inside the connecting volume, spatial average temperatures at the initial and final times for the standard volume delivery apply. Thus,

$$\frac{\rho_{CV_i}}{\bar{\rho}_{MUT}} = 1 + \beta \cdot (\bar{T}_{MUT} - \langle T_{CV_i} \rangle)$$

$$\frac{\rho_{CV_f}}{\bar{\rho}_{MUT}} = 1 + \beta \cdot (\bar{T}_{MUT} - \langle T_{CV_f} \rangle)$$

And

$$\left(\frac{\rho_{CV_i}}{\bar{\rho}_{MUT}} - \frac{\rho_{CV_f}}{\bar{\rho}_{MUT}} \right) = \beta \cdot (\langle T_{CV_f} \rangle - \langle T_{CV_i} \rangle)$$

And from

$$\bar{V}_{MUT} = \bar{V}_{STD} \cdot \left[\frac{\bar{\rho}_{STD}}{\bar{\rho}_{MUT}} + \frac{V_{CV}}{V_{STD}} \cdot \left(\frac{\rho_{CV_i}}{\bar{\rho}_{MUT}} - \frac{\rho_{CV_f}}{\bar{\rho}_{MUT}} \right) \right]$$

$$\bar{V}_{MUT} = \bar{V}_{STD} \cdot \left[1 + \beta \cdot (\bar{T}_{MUT} - \bar{T}_{STD}) + \frac{V_{CV}}{V_{STD}} \cdot \beta \cdot (\langle T_{CV_f} \rangle - \langle T_{CV_i} \rangle) \right]$$

Where

\bar{V}_{MUT} = The time average volumetric flow rate at the meter under test during delivery of the standard volume.

\bar{V}_{STD} = The time average volumetric flow rate at the piston during delivery of the standard volume.

β = The volumetric thermal expansion coefficient of the fluid in the calibration system about the nominal operating temperature at constant pressure.

$$\beta = \frac{1}{V} \frac{\partial V}{\partial T} = - \frac{1}{\rho} \frac{\partial \rho}{\partial T}$$

\bar{T}_{MUT} = The time average temperature at the meter under test during the delivery of the standard volume.

\bar{T}_{STD} = The time average temperature at the piston during the delivery of the standard volume.

V_{CV} = The connecting volume between the meter under test and the piston, the sum of the piping volume from the cylinder discharge port to the meter under test and the volume in the cylinder between the cylinder discharge port and the piston at the end of standard volume delivery.

V_{STD} = The standard volume derived from piston displacement in the cylinder of known cross section.

$\langle T_{CV_f} \rangle$ = The spatial average fluid temperature in the connecting volume at the end of standard volume delivery. Temperature units depend on those of the β being used.

$\langle T_{CV_i} \rangle$ = The spatial average fluid temperature in the connecting volume at the initiation of standard volume delivery. Temperature units depend on those of the β being used.

The final equation,

$$\bar{V}_{MUT} = \bar{V}_{STD} \cdot \left[1 + \beta \cdot (\bar{T}_{MUT} - \bar{T}_{STD}) + \frac{V_{CV}}{V_{STD}} \cdot \beta \cdot (\langle T_{CV_f} \rangle - \langle T_{CV_i} \rangle) \right]$$

consists of three terms when expanded.

The first term, \bar{V}_{STD} , is the average volumetric flow rate at the piston during delivery of the standard volume.

The second term, $\bar{V}_{STD} \cdot \beta \cdot (\bar{T}_{MUT} - \bar{T}_{STD})$ is the same term currently used by existing Air Force calibrators as can be seen when the β -to-density relationship is substituted back in.

$$\bar{V}_{STD} \cdot \beta \cdot (\bar{T}_{MUT} - \bar{T}_{STD}) = \bar{V}_{STD} \cdot \frac{\bar{\rho}_{STD}}{\bar{\rho}_{MUT}}$$

To this point, the two equations are the same – despite one using density and the other using volumetric thermal expansion coefficient.

The third term,

$$\bar{V}_{STD} \cdot \frac{V_{CV}}{V_{STD}} \cdot \beta \cdot (\langle T_{CV_f} \rangle - \langle T_{CV_i} \rangle)$$

is not currently utilized in the Air Force's calibrators. Rather, these calibrators require thermal stability to be achieved to drive this term to zero. When true thermal stability is achieved, this term is not relevant since the initial and final spatial average fluid temperatures will be equal and therefore the entire term will become zero.

Specially Instrumented Positive Displacement Calibrator for Studying Thermal Effects

A representation of the Air Force's current flow calibrator is shown in Figure 2. As can be seen, there are only two temperature measurements made during a standard volume delivery to the meter under test – one is located at the meter under test and the other is located at the inflow directing side of three-way valve upstream of the cylinder. These temperatures are used to correct for the temporal average density difference between the metering piston and meter under test during the time a standard volume is delivered as detailed in the previous section.

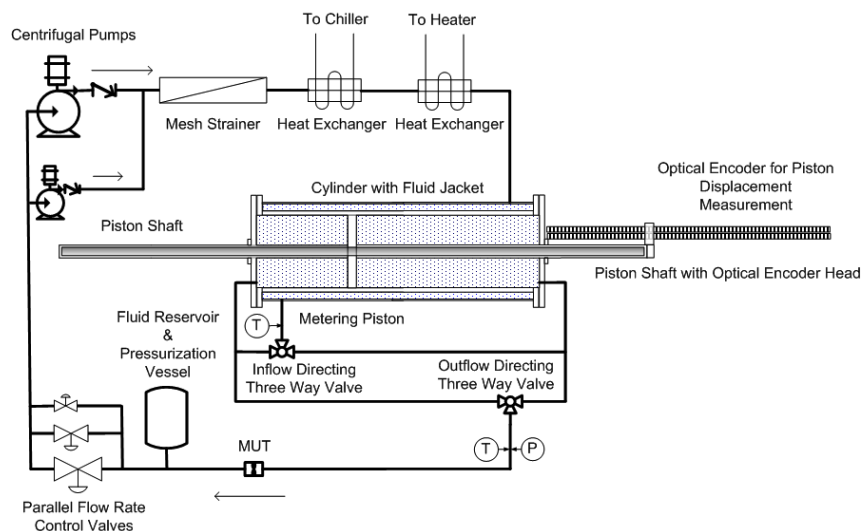


Figure 2: Conventional Bi-Directional piston displacement volumetric flow standard used by the Air Force.

In order to study the effects of assuming thermal stability, we developed a plan for modifying an existing Air Force piston displacement type volumetric flow rate calibrator. This design addressed the issues associated with thermal instabilities – quantification of the spatial average fluid temperature and determination of the connecting volume. Figure 3 depicts this design.

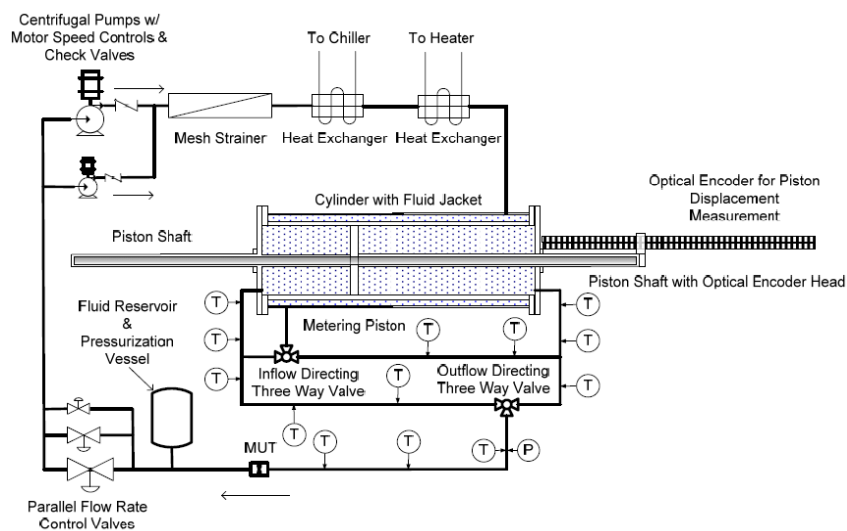


Figure 3: Modified Air Force Bi-Directional piston displacement liquid flow standard.

In order to thoroughly measure the spatial average fluid temperature between the piston and the meter under test, the design called for a total of thirteen thermistor probes – five between the cylinder and meter under test in both directions of piston travel and three in the piping common to both directions of flow. The location of three probes at the pump-end discharge can be seen in Figure 4. A fourteenth thermistor probe was mounted adjacent to the etched glass linear encoder

scale. This allows for application of the glass thermal expansion coefficient to correct for expansion/contraction of the scale.

The design also incorporated a means by which the absolute piston position would be detected, as doing so allows us to quantify the “dead volume” between the metering piston and the cylinder discharge at the end of a standard volume delivery. The software then combines this volume with the piping connecting volume. To achieve this, when the piston reaches the end of its travel and trips the sensor to reposition the three-way valves so that the piston will switch directions, the piston’s position is “zeroed out”. From there, given the number of encoder pulses per unit length, the piston’s distance from the cylinder discharge – and therefore volume between the piston and discharge – can be determined.

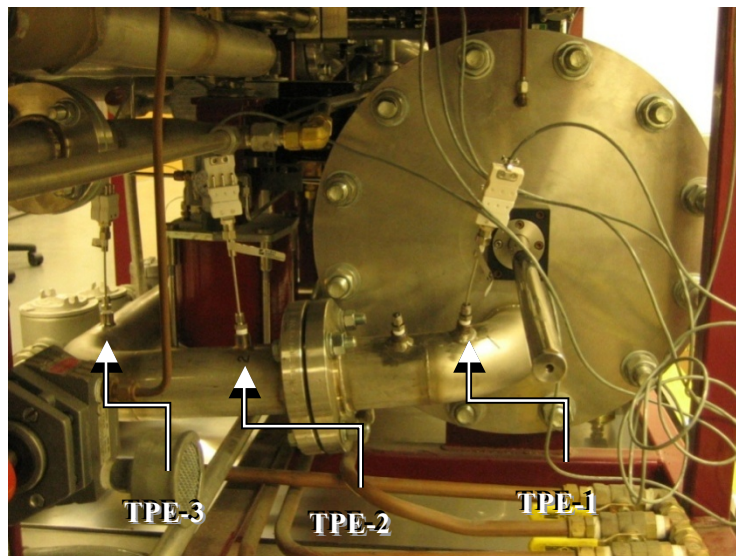


Figure 4: Pump-end temperature probes (TPE-1 through TPE-3) in place during system upgrade.

The calibrator uses small and large centrifugal pumps operated by two different motors. The mode of operation is to turn on the motor, which operates the pump at full speed, and then control to the desired flow rate by way of adjusting three parallel control valves. This means that the work done by the pump on the fluid is about the same for either end of the flow range covered by that pump. For example, the small pump is used for flow rates between 0.5 and 100 GPM; therefore, when operating at flow rates below 100 GPM, unnecessary work is being done on the fluid resulting in fluid temperature increases. To study the effects of this process, we added the ability to control the speed of the two pump motors. Using this option, we can open the three control valves all the way and set flow rates using the variable speed motors. In this scenario, we only transfer the amount of heat as needed to generate the flow rate. This is an option that will be evaluated in the future, with the ultimate plan to move to positive displacement pumps. However, for the testing conducted in this paper, the pumps were operated just as they would be on the conventional calibrator with flow rates being controlled by the control valves.

The fluid used in the modified calibrator was a mixture of propylene glycol and water (15% Propylene Glycol and 85% water).

Evaluating Thermal Instabilities

In order to determine the effect of not accounting for thermal instability, we first tested to determine whether or not thermal instabilities exist. To do this, the temperature term which quantifies thermal instability, $\langle T_{CV_f} \rangle - \langle T_{CV_i} \rangle$, was evaluated under the most common application condition where the fluid is controlled around ambient temperature. If thermal instabilities were found to not exist during standard volume deliveries (i.e. $\langle T_{CV_f} \rangle - \langle T_{CV_i} \rangle$ equals zero), then there would be no need to account for this factor and the current approach to determining average volumetric flow rate delivered to the meter under test would be deemed sufficient.

Fifteen samples were collected for each nominal flow rate stated in Table 2 with a sample time of six seconds, which is equal to 10% of the volume delivered in sixty seconds. The lowest flow rate of 0.7 GPM was selected given that the full range of the test calibrator is 350 GPM. At 0.7 GPM, the turndown is 500:1, and this particular calibrator is specified down to 0.5 GPM. We did not collect data above 200 GPM because the electrical service currently available to the large pump limits operation to 50 amps with the speed control employed. Higher current would be required to pump beyond 200 GPM. Flow rates were generated in the conventional way that these calibrators are operated. This means that the centrifugal pumps are operated at full speed by the motor, and flow rates are set using the three control valves that are in parallel as depicted in Figure 2.

Flow Rate (GPM)	$(\langle T_{CV_f} \rangle - \langle T_{CV_i} \rangle)$ (°F)	$ \langle T_{CV_f} \rangle - \langle T_{CV_i} \rangle $ (°F)	Standard Deviation of $\langle T_{CV_f} \rangle - \langle T_{CV_i} \rangle$ (°F)
0.7	0.000	0.012	0.014
2.5	0.000	0.005	0.006
5.0	0.002	0.008	0.010
10	0.002	0.005	0.008
25	-0.001	0.005	0.007
50	0.001	0.003	0.003
100	-0.001	0.004	0.005
150	-0.021	0.022	0.017
200	-0.021	0.021	0.007

Table 2: Thermal instability data at nominal flow rates.

While not significant in magnitude independently, thermal instabilities do exist. This is believed to be due primarily to the mode of operation in which flow rates are set by control valves while the centrifugal pumps are operated at full speed. This approach results in much work being done on the fluid, thereby heating the fluid and ultimately creating thermal gradients throughout the fluid in the system. This, coupled with heating exchanges with the environment, frictional

heating effects, etc., make it unlikely that true thermal stability will ever be achieved during a standard volume delivery.

Note also the spatial average temperature differences for the 150 and 200 GPM flow rates. These are significantly higher than all of the lower flow rates. This is due to the fact that the large pump was used for the 150 and 200 GPM data points. The data reported for 100 GPM is with the small pump; however, we did run the large pump up at 100 GPM also to evaluate the difference in spatial average temperature differences between the two pumps. The 100 GPM data is stated below in Table 3 while the large pump was used.

Flow Rate (GPM)	$(\langle T_{CV_f} \rangle - \langle T_{CV_i} \rangle)$ (°F)	$ \langle T_{CV_f} \rangle - \langle T_{CV_i} \rangle $ (°F)	Standard Deviation of $\langle T_{CV_f} \rangle - \langle T_{CV_i} \rangle$ (°F)
100	-0.004	0.011	0.017

Table 3: Thermal instability data at 100 GPM using the large pump.

Operating the large pump – as compared to the small pump – multiplied the average magnitude by a factor of nearly three and more than tripled the standard deviation. Use of a pump that is larger than needed for a target flow rate can increase thermal instabilities.

The significance of any thermal instability is that it can ultimately alter flow rates delivered to the meter under test as a result of thermal expansion/contraction. If these instabilities are not accounted for either through the process or uncertainty analysis, additional flow rate errors will arise as a result of small standard volumes (V_{STD}) and/or large connecting volumes (V_{CV}) and/or large volumetric thermal expansion coefficients (β) as explained previously in the derivation of the equation for average volumetric flow rate at the meter under test.

Using the thermal data collected and the additional correction term that accounts for thermal instabilities,

$$\frac{V_{CV}}{V_{STD}} \cdot \beta \cdot (\langle T_{CV_f} \rangle - \langle T_{CV_i} \rangle)$$

the flow rate errors associated with the data recorded above are quantified in Table 4.

Flow Rate (GPM)	Percent Flow Rate Error at Meter Under Test (Average)	Percent Flow Rate Error at Meter Under Test (Average of Absolute Values)	Standard Deviation of Percent Flow Rate Error at Meter Under Test
0.7	0.000	0.084	0.102
2.5	-0.001	0.012	0.015
5.0	0.002	0.011	0.016
10	0.001	0.003	0.005
25	0.000	0.001	0.002
50	0.000	0.000	0.000

100	0.000	0.000	0.000
150	-0.001	0.001	0.001
200	-0.001	0.002	0.002

Table 4: Flow rate errors due to not accounting for thermal instabilities.

The raw data points are presented in chart form in Figure 5.

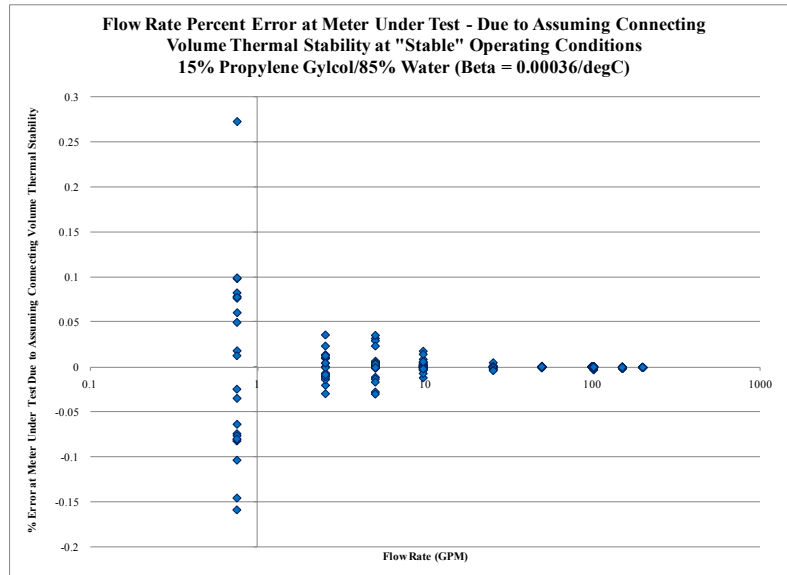


Figure 5: Raw data flow rate errors due to not accounting for thermal instabilities.

As can be seen, the error consequences of not accounting for thermal instabilities increases as flow rate decreases. This is explained knowing that the thermal instability term $\langle T_{CV_f} \rangle - \langle T_{CV_i} \rangle$ is magnified based on the ratio of connecting volume to standard volume

$$\frac{V_{CV}}{V_{STD}} \cdot \beta \cdot (\langle T_{CV_f} \rangle - \langle T_{CV_i} \rangle)$$

When flow rates decrease, the likelihood increases that the standard volume delivery will begin and end far away from the cylinder discharge and that the standard volume will decrease, thereby increasing the connecting volume. This results in making the ratio of $\frac{V_{CV}}{V_{STD}}$ larger for low flow rates as compared to higher flow rates.

Reducing Flow Rate Errors Associated with Thermal Instabilities through Increased Standard Volume Sizes

Given the average volumetric flow rate errors at the meter under test associated with not accounting for thermal instabilities in the connecting volume during standard volume delivery, we explored the reduction of these errors by increasing standard volume, V_{STD} , sizes (i.e. increased collection times). The basis for this is that the previously derived relationship

indicates that an increase in V_{STD} can result in a decrease to the $\frac{V_{CV}}{V_{STD}}$ term and therefore a decrease in error for a given thermal instability.

These tests were conducted at three focus flow rates, 25, 5 and 0.7 GPM given the results of the above thermal studies which indicated the most significant errors occurred at the lower flow rates.

A minimum of 100 data points were collected at each of these flow rates for four different standard volume sizes, V_{STD} , related to 6, 15, and 30 seconds; 10 data points were collected for the 60 second standard volume equivalent. The objective was to understand the real effect on average volumetric flow rate delivered to the meter under test as a function of varying standard volume sizes. This information could be used to reduce the effect of thermal instability errors in those labs operating this style of calibrator with no real capital expense.

The following three graphs (Figures 6 through 8) display the results.

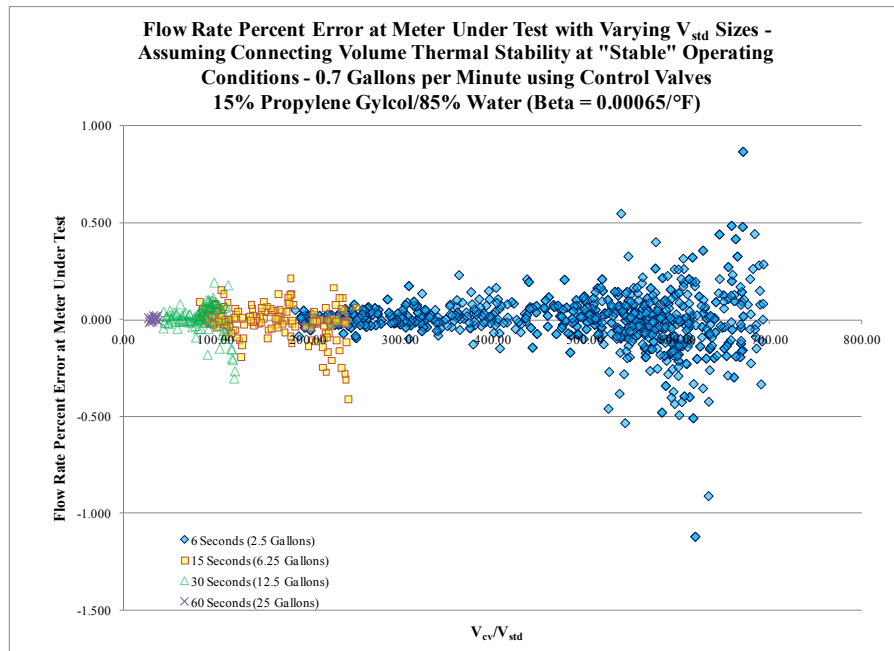


Figure 6: Flow rate percent error at meter under test at 0.7 GPM with varying V_{std} .

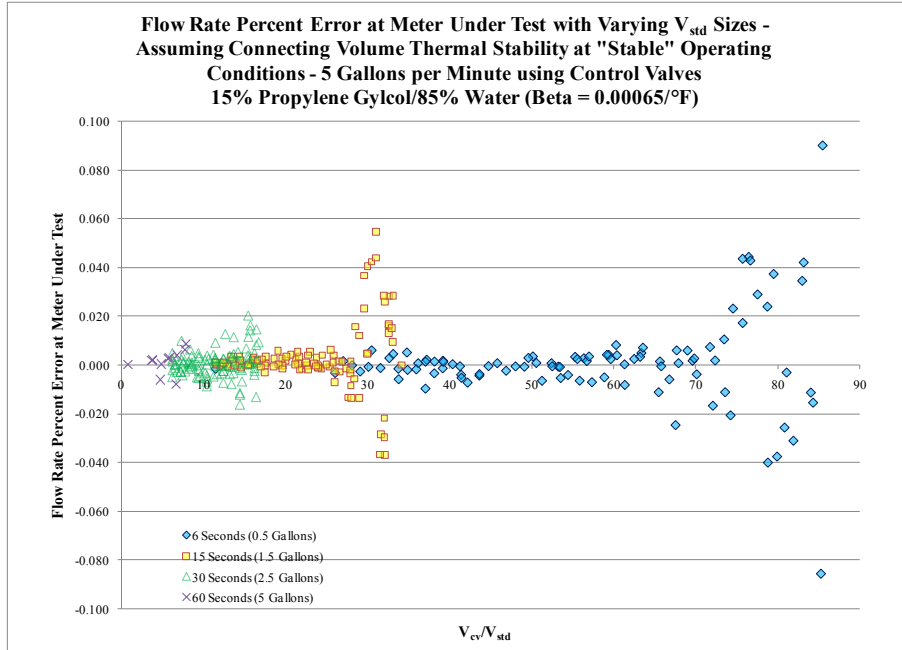


Figure 7: Flow rate percent error at meter under test at 5 GPM with varying V_{std} .

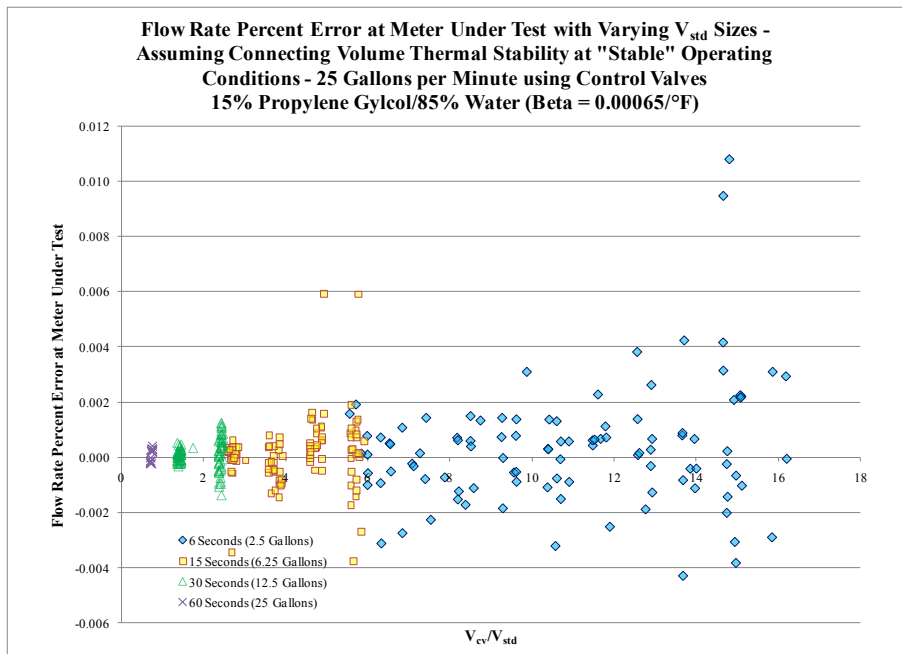


Figure 8: Flow rate percent error at meter under test at 25 GPM with varying V_{std} .

These data provide further quantifiable justification for the need to account for thermal instabilities during standard volume deliveries. First, having now collected over one thousand data points, it is even clearer that thermal instabilities do exist given the quantities of non-zero flow rate errors. Second, the errors center on zero error. This means that controlling temperature around ambient – as we did – can be nominally effective, but there will always be

“thermal noise” in spatial average temperature between the end and beginning of a standard volume delivery; it cannot be controlled away completely. Third, as standard volume sizes increase (i.e. the sample time increases), the errors associated with not accounting for thermal instabilities decrease. The explanation again revolves around the ratio of connecting volume and standard volume, $\frac{V_{CV}}{V_{STD}}$, and that by increasing V_{STD} , the term magnitude – and therefore associated flow rate errors – can be reduced for a given value of $\langle T_{CV_f} \rangle - \langle T_{CV_i} \rangle$. Fourth, the data takes on a “trumpet horn” profile moving to the right as the ratio of $\frac{V_{CV}}{V_{STD}}$ increases. Having taken so many data points, the shape forms as a result of high $\frac{V_{CV}}{V_{STD}}$ ratios coupled with the higher thermal instability magnitudes during standard volume deliveries.

The tables below (Tables 5 through 8) summarize the statistics associated with the testing in this section. The lower and upper confidence levels are provided to put the errors into statistical context. Note, however, that this confidence interval is based on all data collected in this section and therefore does reflect improvements that would be realized by increasing connecting volume to standard volume ratios.

Flow Rate (GPM)	Average Error (%)	Absolute Error (%)	Standard Deviation (%)	LCL (95%)	UCL (95%)
0.7	0.000	0.087	0.142	0.284	-0.284
5	0.001	0.010	0.019	-0.037	0.039
25	0.000	0.001	0.002	-0.004	0.005

Table 5: Statistics for data collected with a standard volume sample time of 6 seconds

Flow Rate (GPM)	Average Error (%)	Absolute Error (%)	Standard Deviation (%)	LCL (95%)	UCL (95%)
0.7	-0.010	0.062	0.090	-0.191	0.171
5	0.003	0.008	0.014	-0.025	0.031
25	0.000	0.001	0.001	-0.002	0.003

Table 6: Statistics for data collected with a standard volume sample time of 15 seconds

Flow Rate (GPM)	Average Error (%)	Absolute Error (%)	Standard Deviation (%)	LCL (95%)	UCL (95%)
0.7	0.003	0.051	0.074	-0.145	0.151
5	0.001	0.004	0.006	-0.011	0.013
25	0.000	0.000	0.000	-0.001	0.001

Table 7: Statistics for data collected with a standard volume sample time of 30 seconds

Flow Rate (GPM)	Average Error (%)	Absolute Error (%)	Standard Deviation (%)	LCL (95%)	UCL (95%)
0.7	0.003	0.009	0.010	-0.017	0.024
5	0.001	0.004	0.005	-0.008	0.011
25	0.000	0.000	0.000	0.000	0.001

Table 8: Statistics for data collected with a standard volume sample time of 60 seconds

Conclusions and Recommendations

We conclude from our testing that thermal stability cannot truly be achieved and that thermal instabilities do exist in the connecting volume during standard volume deliveries (where connecting volume is defined as the volume between the meter under test and the metering piston's final location in the cylinder). Further, the magnitudes of these thermal instabilities are significant enough that not accounting for them will lead to non-negligible flow rate errors at lower flow rates. This is true because changes in spatial average temperature lead to net thermal energy gains/losses and therefore decreases/increases in volumetric flow as a result of fluid contraction/expansion.

In order to most accurately measure average volumetric flow rate at the meter under test, we recommend use of the full equation derived above and re-stated below.

$$\bar{V}_{MUT} = \bar{V}_{STD} \cdot \left[1 + \beta \cdot (\bar{T}_{MUT} - \bar{T}_{STD}) + \frac{V_{CV}}{V_{STD}} \cdot \beta \cdot (\langle T_{CV_f} \rangle - \langle T_{CV_i} \rangle) \right]$$

This formula properly accounts for the thermal “storage effects” that occur during standard volume deliveries, whereas the conventional “two term” formula

$$\bar{V}_{MUT} = \bar{V}_{STD} \cdot [1 + \beta \cdot (\bar{T}_{MUT} - \bar{T}_{STD})]$$

does not as a result of assuming thermal stability.

We also conclude that thermal errors cannot be controlled away. The data presented indicates that even when controlling at ambient temperature – as we did in these studies – there will still be differences in the spatial average temperature between the beginning and end of a standard volume delivery.

Obviously, the best way to avoid thermal instability effects is to achieve and maintain steady state during standard volume deliveries; however, when a heat producing pumping process is involved or controlling fluid temperature at some level different from that of the ambient surroundings, thermal stability can be elusive. Instigating the ability to measure and account for thermal instability can be a process improvement of merit. Other methods also exist for minimizing the impact of thermal instability on the uncertainty of flow rates delivered to a meter under test.

In order to decrease these effects, Table 9 is first provided to define the three contributory variables, along with their relationship to flow rate, and how these can be maintained.

Variable	Relationship to Flow Rate	Action to Counter Thermal Instability Effects
V_{CV} , Connecting Volume	An <i>increase</i> in V_{CV} increases the	The connecting volume is a function of where the metering piston completes its standard volume

	effect of thermal instability	delivery. As the piston moves closer to the cylinder discharge, the smaller V_{CV} becomes. Operating the flow calibrator to have the piston complete its standard volume delivery close to the cylinder discharge will decrease the effects of thermal instability.
V_{STD} , Standard Volume Delivered	A decrease in V_{STD} increases the effect of thermal instability	The standard volume term is a function of the volume collected for an average volumetric flow rate. Increasing the size of the standard volume decreases the effects of thermal instability.
β , Fluid Volumetric Thermal Expansion Coefficient	An increase in β increases the effect of thermal instability	The volumetric thermal expansion coefficient is a function of the calibrator's fluid. Fluids with a smaller expansion coefficient will decrease the effects of thermal instability. A lot of flow calibrators use Stoddard Solvent. A proposed alternative is mixtures of Propylene Glycol and water. The volumetric thermal expansion coefficient of 15-percent Propylene Glycol and 85-percent water is almost three times smaller than that of Stoddard Solvent at ambient temperature.

Table 9: Summary of contributory variables and actions to reduce flow rate errors associated with not accounting for thermal instabilities.

These are turnkey steps that can be taken to immediately reduce the impact of thermal instabilities. There are, however, other factors to be considered.

These calibrators are typically specified with a low uncertainty over a wide turndown – sometimes up to 1,000:1. The data presented in this paper indicate that without accounting for thermal instabilities, the lower range flow rates can be significantly impacted. For example, a 0.7 GPM flow rate (at the 500:1 turndown) of 15-percent Propylene Glycol and 85-percent water and a standard volume collection time of 15 seconds can lead to errors of approximately $\pm 0.2\%$ of flow rate. Determining a sufficient turndown limitation based on needs can reduce the impact, perhaps without capital investments for accounting for these effects and/or without needing to alter established calibration procedures.

Some of these calibrators will operate with two differently sized pumps to cover the entire flow range. Choosing the smallest pump for the desired flow rate can reduce the thermal impact on the fluid and therefore minimize errors.

A fluid's specific heat capacity is also relevant since the amount of energy required to change the fluid's temperature will vary from fluid to fluid. Therefore, the work done on the fluid by the pumps can change the temperature of two fluids differently.

Lastly, when using heat exchangers to alter the fluid's target temperature (different than controlling at an already-established target temperature), allow sufficient time for the fluid to

circulate through the system and stabilize around the nominal temperature. Changing the target temperature of the fluid followed by data collection shortly thereafter may result in abnormally large thermal instability effects and therefore unintended flow rate errors.

Future Studies

The tests described in this paper will be repeated in the future to further optimize the process improvement concepts. Such endeavors include use of the variable speed motors and eventually positive displacement pumps in order to reduce the heat transferred to the fluid during the pumping process. We also plan to study the number of and locations of the temperature probes needed in order to obtain a sufficient thermal map of the connecting volume for spatial average temperature determination. This will make implementation of this approach more practical, affordable, and maintainable.

References

T.T. Yeh, Jesús Aguilera, and John D. Wright, "Hydrocarbon Liquid Flow Calibration Service, NIST Special Publication 250-1039."

T.T. Yeh, P.I. Espina, G.E. Mattingly, and N.R. Briggs, "An Uncertainty Analysis of a NIST Hydrocarbon Liquid Flow Calibration Facility," Proceedings of HT/FED'04 2004 Heat Transfer/Fluids Engineering Summer Conference, 2004, Published by the American Society of Mechanical Engineers.